SPECKLE NOISE REDUCTION USING ADAPTIVE MULTISCALE PRODUCTS THRESHOLDING

By

NUR ARASH BT BUKHARI

FINAL PROJECT REPORT

Submitted to the Department of Electrical & Electronic Engineering in
Partial Fulfillment of the Requirements for the Degree
Bachelor of Engineering (Hons)
(Electrical & Electronic Engineering)

Universiti Teknologi PETRONAS
Bandar Seri Iskandar
31750 Tronoh
Perak Darul Ridzuan

CERTIFICATION OF APPROVAL

SPECKLE NOISE REDUCTION USING ADAPTIVE MULTISCALE PRODUCTS THRESHOLDING

by

Nur Arash Bt Bukhari
13312

A project dissertation submitted to the
Department of Electrical & Electronic Engineering
Universiti Teknologi PETRONAS
in partial fulfillment of the requirement for the
Bachelor of Engineering (Hons)
(Electrical & Electronic Engineering)

Approved by,

_____

(Ms. Norashikin Bt Yahya)
Project Supervisor

UNIVERSITI TEKNOLOGI PETRONAS
TRONOH, PERAK

January 2014

CERTIFICATION OF ORIGINALITY

This is to certify that I am responsible for the work submitted in this project, that the original work is my own except as specified in the references and acknowledgements, and that the original work contained herein have not been undertaken or done by unspecified sources or persons.

_____

(NUR ARASH BT BUKHARI)

ABSTRACT

Image denoising is an essential preprocessing technique in image acquisition systems. For instance, in ultrasound (US) images, suppression of speckle noise while preserving the edges is highly preferred. Thus, in this paper denoising the speckle noise by using wavelet-based multiscale product thresholding approach is presented. The underlying principle of this technique is to apply dyadic wavelet transform and performs the multiscale products of the wavelet transform. Then, an adaptive threshold is calculated and applied to the multiscale products instead of applying it on wavelet coefficient. Thereafter, the performance of the proposed technique is compared with other denoising techniques such as Lee filter, boxcar filter, linear minimum mean square error (LMMSE) filter and median filter. The result shows that the proposed technique gives a better performance in terms of PNSR and ENL value by an average gain of 1.22 and 1.8 times the noisy on, respectively and can better preserved image details.

ACKNOWLEDGEMENT

First of all, thanks to Allah SWT, with His willing and blessing I was able to complete this Final Year Project entitles 'Speckle Noise Reduction using Adaptive Multiscale Products Thresholding'.

My appreciation and gratitude goes to my supervisor, Ms. Norashikin Yahya, for her sincere guidance, advice and support throughout the whole period of Final Year Project. She has constantly provided valuable knowledge since the beginning of the project until the completion of this dissertation. I believed the success of this project would not be possible without her involvement and contribution. Besides, I would like to thank Department of Electrical and Electronic Engineering, Universiti Teknologi PETRONAS for giving me the opportunity to execute this project.

Finally, I would like to express my gratitude to my beloved family for their blessing and everyone that gave me unconditional support and encouragement to complete my Final Year Project. A warm thanks to my fellow friends in making my work a great success. Thank you.

TABLE OF CONTENTS

LIST OF TABLE

LIST OF GRAPH

LIST OF FIGURE

LIST OF ABBREVIATIONS

US	Ultrasound
DWT	Dyadic Wavelet Transform
AMPT	Adaptive Multiscale Product Thresholding
LMMSE	Linear Minimum Mean Square Error
PSNR	Peak-signal-noise-to-ratio
ENL	Equivalent Number of Look
MAD	Median Absolute Deviation

CHAPTER 1

INTRODUCTION

In this chapter, the first section covered the background study of US images including the underlying principle of US imaging technique and the statistic of speckle noise. In the subsequent sections, the problem statement, objective and scope of the project are elaborated in detail.

1.1 Background of Study

In medical image processing, Ultrasound (US) imaging is a technology that uses high-frequency of sound waves. In an ultrasound-based diagnostic technique or also known as ultrasonography, a hand-held transducer is used to visualize soft tissues such as muscles and internal organs in a real time imaging. The transducer which is placed against the patient's skin will transmitted the sound waves into the body structures and the reflected waves or echoes are displayed as an image. Basically, US imaging are signal which are obtained by coherent summation of echo signals that scattered in the tissues [2]. This technology is easy, inexpensive and is a safe medical diagnostic technique. Fig 1 illustrated the application of ultrasonography in medical world. The physician is using US technology to examine the condition of the pregnant lady and her fetus.

Figure 1: Ultrasonography Examination [1]

The formation of US images by mean of coherent processing of the returned backscattered signals, introduces speckle effect in the images. Speckle noise is a multiplicative noise that appears in the form of a random granular pattern that delays the interpretation of the image contents [3]. Speckle effect lessens the resolution of the image generated and makes it blurred. Besides, it intricate the diagnosis of image edge detection and image segmentation [4]. Modeling of speckle noise in ultrasound images can be expressed as

$$f = g\eta\,, \tag{1}$$

where f is the speckle noise matrix, g is the noise-free ideal image and η is the unit of random variable speckle noise matrix that follows Rayleigh distribution. Assuming the speckle is fully formed, the probability density function (pdf) of the noise is given by

$$P_R(r) = \frac{r}{v^2}\ \exp\left(-\frac{\mathrm{r}^2}{2\mathrm{v}^2}\right),\ r \geq 0\,, \tag{2}$$

where r is real. To convert the multiplication model of (1) to additive model, we apply logarithmic transform to (1) giving

$$\log(f) = \log(g) + \log(\eta)\ . \tag{3}$$

Expression (3) can be rewritten as

$$f_l = g_l + \varepsilon_l\ . \tag{4}$$

Denoising the speckle by smoothing or averaging process is not the best option as it will destroy some important features of the image. Therefore, it is essential to choose the most effective technique to despeckle the noise while preserving the image details such as edges and texture. In this project, Adaptive Multiscale Product Thresholding technique [5] is proposed to reduce speckle noise in ultrasound images. The result from this technique will be compared with commonly adaptive filter, such as Lee filter, boxcar filter, linear minimum mean square error (LMMSE) filter and median filter. For the evaluation, peak signal-to-ratio (PSNR) will be used as the quantitative measure for the filters performance.

1.2 Problem Statement

Ultrasound (US) images suffer from speckle effect due to the coherent processing of the return backscattered signals. Although, noise can be reduced by improving the imaging acquisition hardware, in the case of US imagery, the speckle is the type of noise that forms during the image acquisition process. Therefore, US images need to be post-processed by some noise removal technique before any subsequent image processing operations. In this project, speckle noise reduction using Adaptive Multiscale Products Thresholding is employed. The significant of this project is to enhance the reduction of speckle noise in US by suppressing the noise and preserving the image details.

1.3 Objective

Basically, the main objective of this project is to implement and evaluate the speckle reduction technique based on Adaptive Multiscale Product thresholding technique.

The scope of this project includes:

- Study and analysis of speckle formation and speckle statistic in US images
- Study and analysis of common speckle filters such as Lee, Kuan, and Frost
- Study and analysis of Adaptive Multiscale Product Thresholding filter which was originally developed for additive noise [5].
- Develop a speckle filter based on Adaptive Multiscale Product Thresholding (AMPT) technique.
- Evaluate and compare the performance of the speckle filter.

CHAPTER 2

LITERATURE REVIEW

In this chapter, the first section covered the adaptive filters that are commonly used in despeckling the noise. In the subsequent sections, wavelet transform and proposed technique, adaptive multiscale product thresholding are discussed in detail.

2.1 Adaptive Filter

Filtering is one of the methods used in reducing speckle noise. The adaptive filter designs itself within a window based on the statistical characteristic of the input signal inside the filter. The estimated statistical information is a local mean and local variance which resemble the average gray level of the pixel and the average contrast of the pixel respectively [6]. Adaptive filtering techniques that commonly used are Lee filter, Kuan filter, Frost filter, enhanced Lee and Frost filter, and median filter. Lee and Kuan filter use a linear combination of the center pixel intensity in a filter window with the average intensity of the window to generate an output image. Frost filter is an exponential shaped filter kernel that computes a set of weight value for each pixel within the filter [2]. Median filter is a best non-linear filter which replaces each point in the window with the median value of the corresponding neighborhood. In adaptive median filter, it works by increasing the rectangular window area until maximum window size is achieved [6]. Linear minimum mean square (LMMSE) and boxcar filter are another example of commonly used filter. Boxcar filter is a low pass filter and it works by moving an average of some number of time sample, where each sample are equally affect the output produced. In [7], LMMSE technique used by Zhang to estimate the missing sample for denoising while performing interpolation shows an impressive result. Table 1 below shows the summary of each adaptive filters performance.

Table 1 : Summary of Adaptive Filter

No	Type of Filter	Features
1.	Lee Filter	• Smoothens the background noise effectively but tend to ignore the speckle noise in the area closest to edges and lines and causes blurring effect
2.	Enhanced Lee Filter	• Smoothens the background noise more effectively compared to Lee filter • Retains edges and sharp features in the image but some point targets are not detected and usually get blurred
3.	Frost Filter	• Filtering technique based on pixel distances to correct multiplicative noise while retaining edges and other object • Act as a mean filter for uniform regions and high pass filter for high contrast regions • Produces outputs approximately similar to Lee and Kuan filter
4.	Enhanced Frost Filter	• Filtering based on neighboring distances of the centre pixels and be able to preserve edges better compared to others • If the kernel size is small, the filtering is not effective whereas if the kernel size is too large, subtle details of the image are lost
5.	Kuan Filter	• Smoothens the background noise effectively and better preservation of edges and sharp features compared to Lee filter
6.	Boxcar Filter	• Simple to apply and reduce speckle noise in homogeneous areas effectively while preserving the mean value but tend to degrade the spatial resolution and causes blurring effect
7.	Median Filter	• Moderately effective in reducing speckle effect but tend to cause distortion and fail to preserve the mean value
8.	Linear Minimum Mean Square (LMMSE)	• Moderately effective in reducing speckle effect but the speckle noise is not adequately filter near strong edges of the image

2.2 Wavelet Transform

Denoising technique based on wavelet transform continue to receive great attention among the image processing community. Features of wavelet transform such as multiresolution, sparsity, edge detection and edge clustering make the application of wavelet transform as a speckle noise reduction technique to be more appealing compared to the common adaptive filters. In the conventional approach of speckle filter, a large size of window is used and this will reduce the resolution of the algorithm [3]. On the other hand, in wavelet transform, signal is analyzed with a short window at high frequency and long window at low frequency. Thus, the noise and actual image can be distinguished easily at different multiresolution.

Discrete wavelet transform is an expansion of wavelet series that has been discretely sampled. Discrete wavelet transform is an expansion of wavelet series that has been discretely sampled. The discrete wavelet transform consists of high pass and low pass filter which provide details information and coarse scale approximation, respectively. The decomposition of these two filters is based on Mallat algorithm. At each level, the half band filter produces signals within half of the frequency band. Thus, it doubled the frequency resolution as the frequency is reduced by half. Output of the low pass filter will produced approximation coefficient whereas output of high pass filter will produced details coefficient, followed in both cases with decimation by 2. This decimation by 2 reduced the time resolution by half [8]. With the existence of these two filters, the time resolution increase at high frequency while frequency resolution increase at low frequency. In Fig.2 shows the two-level of decomposition that has been replaced with four blocks which correspond to the low pass and high pass subbands.

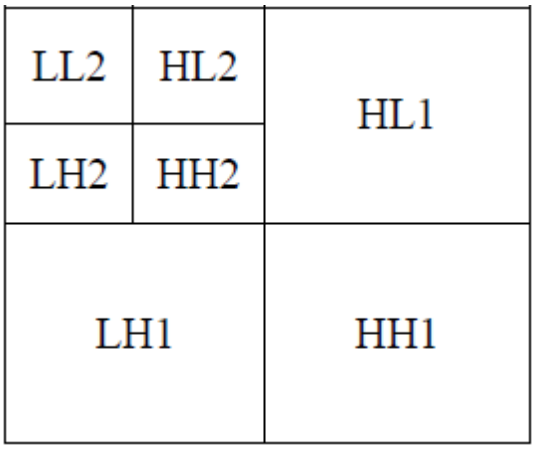

Figure 2: Two-level image decomposition by using discrete wavelet transform [3]

Dyadic Wavelet Transform (DWT) is a scale sample of wavelet transforms that follow geometric sequence of ratio 2. The DWT is a redundant wavelet transforms which provide a longer length of transform coefficients compared to the original signal. Thus, it increases the sampling for the time frequency plane and gives good shift invariance [9]. The characteristics of DWT will enhance the quality of image during reconstruction and give better performance compared to discrete wavelet transform. Fig. 3 shows the decomposition and reconstruction algorithm of dyadic wavelet transform.

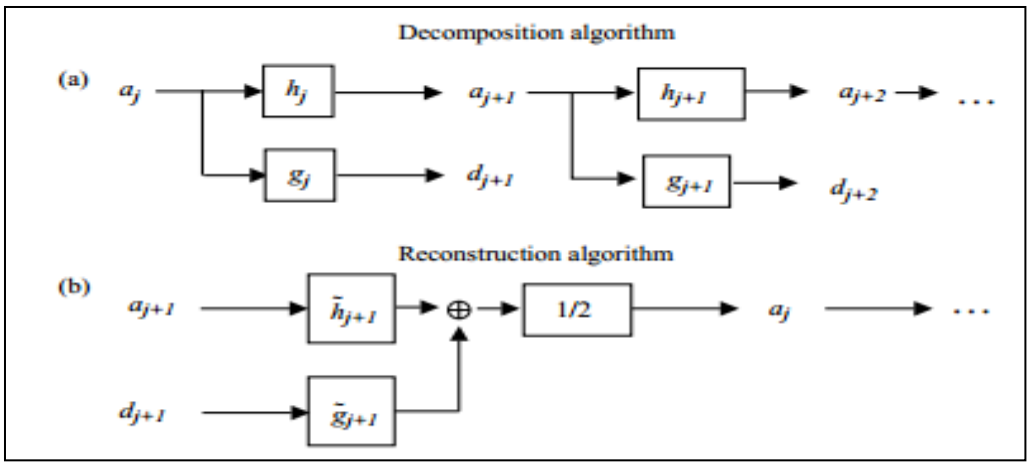

Figure 3 : Fast algorithm of dyadic wavelet transform. a) Decomposition b) Reconstruction [10]

2.3 Adaptive Multiscale Products Thresholding

Wavelet based thresholding scheme for speckle reduction have been proposed and proved to be effective by a number of authors [5, 11-14]. The basic idea of threshold is to set or shrink the input wavelet coefficient. This is known as soft thresholding technique. Universal threshold [15] and BayeShrink threshold [12] are example of soft threshold scheme which is based on orthogonal wavelets . In contrary, hard thresholding technique will retain the input wavelet coefficient if it is greater than the threshold. In [16], Pan et al. used this technique and applied it to nonorthogonal wavelet transform. Typically, all proposed wavelet threshold schemes implemented the threshold technique directly to the wavelet coefficient.

The thresholding technique was later improved by a comparative study and analysis of multiscale product of wavelet subbands and it results in a more distinguishable structure between edges and noise [17, 18]. By exploiting the singularities of signal and dependency between the wavelet subband, the original signal and noise can be distinguished easily. This is because, in the wavelet transform, signal and noise appear and behave differently. Fig 4 shows the sequence of signal and noise in wavelet transform domain. Here, singularity of a signal refers to a point at which a function has an interrupted point and possesses a zero-derivative almost everywhere. Singularity of a function is discontinuous at its singular points. Conversely, a function which has an infinite-order derivative and it is continuous are known as smooth function or not singular. The singularity of a signal can be analyzed by mathematical concept of the Lipschitz regularity. White noise has singular properties everywhere and has a uniform negative Lipschitz regularity that is equivalent to -1/2. Based on Lipschitz regularity concept, magnitude of wavelet transform increase for positive Lipschitz regularity with increasing scales. Conversely, magnitude wavelet transforms decrease for negative Lipschitz regularity with increasing scales.

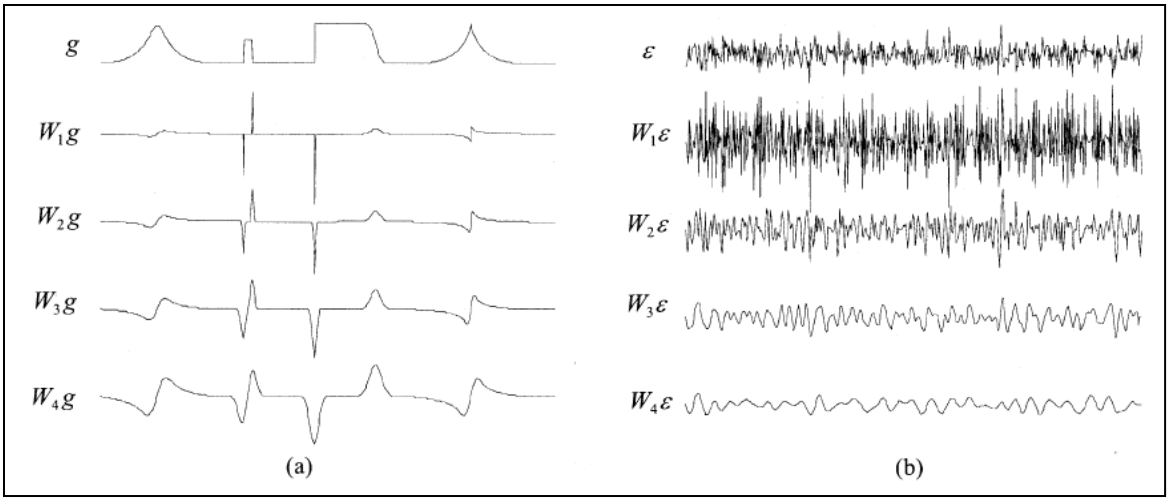

Figure 4: (a) DWT of test signal, g at the first four scale (b) DWT of Gaussian white noise, ε at the first four scales [5]

As illustrated in Fig 4, the singularities of signal increase across the scale while the magnitudes of noise start to decay along scales. Prior to this knowledge, multiplying the DWT at adjacent scale will enhance the structure of the signal while diluting the noise. In [5], Zhang proved that even though the original signal are immersed into the noise at fine scale but the original signal is enhanced by multiplying the DWT at adjacent scales. Fig 5 illustrated the DWT and multiscale products of a noisy test signal. In Fig 5, *f* is the noisy signal and *Wif* corresponds to the *i th*-wavelet level. The *Pif* is the product between *i th* wavelet level and *Wif.*

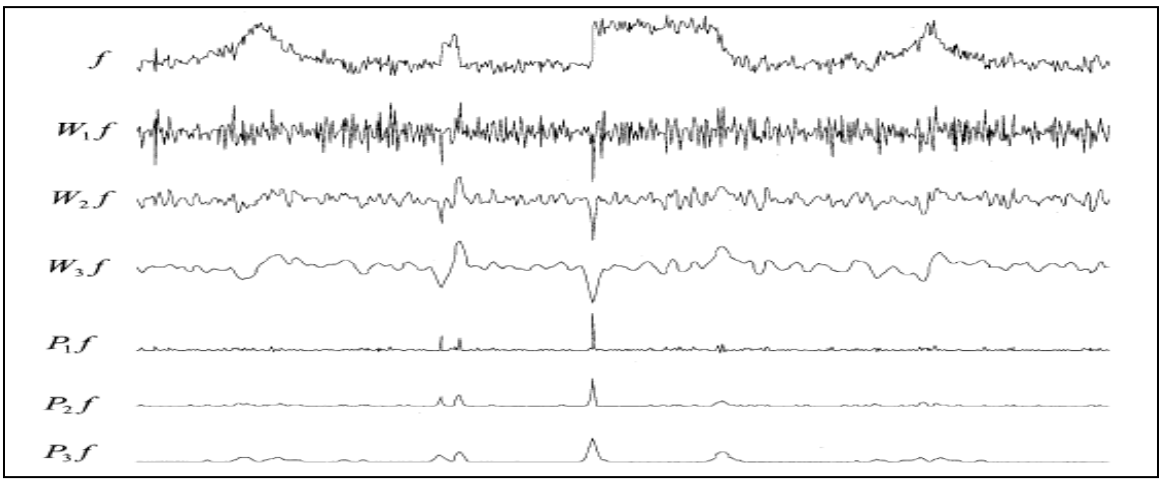

Figure 5: The DWT and multiscale products of noisy test signal at the first three scales [5]

Fig 6, 7, 8 and 9 shows the decomposition of a test image which has been corrupted with a noise variance of 40 with increasing wavelet scales from scale one up to scale four. From these figure, one can clearly observed that along the scales, the noise are reduced and the image are smoothened. The degree of smoothness increase rapidly with increasing scales but the images become too smooth and cause blurring effect. The smoothed image resulted from decomposition of DWT. Besides, the performance metric, PSNR values tend to reduce as the scale increases. The average PSNR value of noisy image is 16.07 and the PSNR values of smoothed image at the first four wavelet scale are 24.68, 23.89, 21.22 and 19.25, respectively. Notice that the PNSR values obtained are inversely proportional to the wavelet scales. With this observation, the property of noise with respects to Lipschitz regularities is proven.

Figure 6: The DWT of noisy House image at scale one.
(a) Noise-free image. (b) Noisy image (PNSR=16.06). (c) Smoothed image (PNSR=24.68).

(a) (b) (c)

Figure 7: The DWT of noisy House image at scale two.
(a) Noise-free image. (b) Noisy image (PNSR=16.07). (c) Smoothed image (PNSR=23.89).

(a) (b) (c)

Figure 8: The DWT of noisy House image at scale three.
(a) Noise-free image. (b) Noisy image (PNSR=16.08). (c) Smoothed image (PNSR=21.22).

(a) (b) (c)

Figure 9: The DWT of noisy House image at scale four.
(a) Noise-free image. (b) Noisy image (PNSR=16.10). (c) Smoothed image (PNSR=19.25).

Thus, in this work we favor multiscale product thresholding scheme to reduce speckle noise in ultrasound images. Assuming speckle noise in log-domain to be approximately Gaussian white noise, the Gaussian additive model ($f = g + \varepsilon$) is adopted and the DWT of the noise, can be expressed as [5]

$$W_j^d f = W_j^d g + W_j^d \varepsilon \ , \ (d = x, y), \tag{5}$$

where $W_j^d g$ is the DWT of the original image g and $W_j^d \varepsilon$ is the DWT of additive noise ε. The notation $d = x, y$ indicates x or y dimension. The multiscale product, $P_j^d f$ is the product between two adjacent wavelet scales. Z_j^d is a simple expression for the multiscale product of noise given as

$$Z_j^d = P_j^d f = W_j^d f . W_{j+1}^d f \ . \tag{6}$$

Here, high dependencies exists between $W_j^d f$ and $W_{j+1}^d f$. The standard deviation of multi-scale product of noise can be denoted as [14]

$$k_j^d = \sqrt{E\left[\left(W_j^d \varepsilon\right)^2 \left(W_{j+1}^d \varepsilon\right)^2\right]} = \sqrt{1 + 2\left(p_{j+1}\right)^2} . \sigma_j \sigma_{j+1} \ , \tag{7}$$

where p_{j+1} is the correlation coefficient and σ_j is the standard deviation of Gaussian white noise. The adaptive threshold can be calculated by using the expression

$$t_j^d = 5k_j^d \left(1 + \frac{\mu_j^d \varepsilon}{\mu_j^d g}\right) , \tag{8}$$

where $\mu_j^d \varepsilon$ is the mean value of multiscale product of Gaussian noise and $\mu_j^d g$ is the mean value of multiscale product of the original image. Based on calculated value in equation (8), multiscale products is thresholded by

$$\widehat{W}_j^d f = \begin{cases} W_j^d f & P_j^d f \geq t_j^d(j) \\ 0 & P_j^d f < t_j^d(j) \end{cases} , j = 1, \ldots J; d = x, y. \tag{9}$$

Significant wavelet coefficients which are greater than the preset threshold are preserved and the image will be reconstructed from this thresholded wavelet coefficients, $\widehat{W}_j^d f$. Otherwise, anything below the threshold value are set to zero and discarded as noise.

CHAPTER 3

METHODOLOGY

In this section, the algorithm of AMPT technique and noise level estimator used in this technique is further elaborated. The experiments is carried out in MATLAB in order to investigate the performance of proposed technique using synthetically speckled test images and real US images. The wavelet transform used in this technique is based on Dyadic Wavelet Transform (DWT). The dyadic wavelet constructed by Mallat and Zhong [19] is employed in the AMPT technique. This wavelet is basically originated from the mother wavelet of a quadratic spline wavelet.

3.1 Adaptive Multiscale Product Thresholding Image Denoising Technique

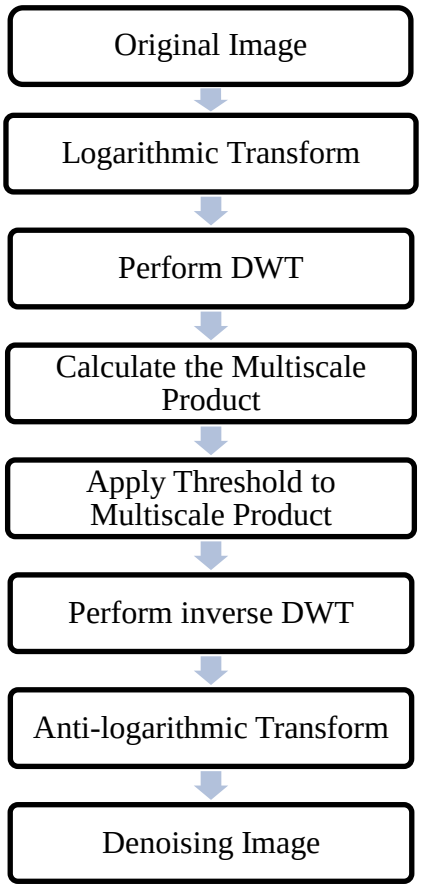

Figure 10: Adaptive Multiscale Product Thresholding (AMPT) Scheme

Figure 10 shows the methodology of the proposed technique. Firstly, logarithmic transform is applied to speckle model in order to convert from multiplication model to additive model. After that, the DWT is computed on the original image up to a few scales. Then, multiscale products of DWT is calculated by multiplying two adjacent of wavelet subbands to preserve edge structures while diluting the noise. An adaptive threshold is calculated and applied to the multiscale products instead of applying it on wavelet coefficient. This is because the multiscale thresholding products can distinguish edge structures from noise better compared to threshold wavelet coefficient. Lastly, inverse DWT is performed to reconstruct the denoised image and anti-logarithmic transform is applied.

3.2 Estimation of Noise Variance

The term noise variance is referring to the noisy level of the image. In order to execute denoising scheme, it is essential to have the accurate information regarding the noise level present in the image. The noise level can be estimated based on information other than the corrupted image. By using robust median estimator proposed by Donoho [15], the noise level is measured in the highest subband of wavelet transform, HH_1. Robust median estimator is a common noise estimation used in the wavelet domain by computing the noise standard deviation as the median absolute deviation (MAD) of the wavelet coefficient. The estimation of variance is given by

$$\vartheta_n = median\left(\frac{|Y(i,j)|}{0.6745}\right),\ Y(i,j) \in subband\ HH_1. \quad (9).$$

For AMPT technique, the calculated variance in equation (9) is estimated as standard deviation of additive Gaussian white noise, σ_j and used in equation (7). The standard deviation is denoted by

$$\sigma_j = \vartheta_n\ . \quad (10).$$

CHAPTER 4

RESULTS AND DISCUSSIONS

The results presented in this section are divided into two major sections, firstly using simulated data and secondly using real US images. The performance metric used in the simulated data is peak-signal-to-noise ratio (PSNR) whereas in the real US images, the equivalent number of look (ENL) is used to measure the amount of noise reduction in the filtered image. The PSNR is defined as equation [3]

$$PNSR = 10\log_{10}\frac{255}{MSE}\ , \tag{9}$$

$$MSE = \frac{1}{MN}\sum_{i=1}^{M}\sum_{j=1}^{N}\big(X(i,j) - Y(i,j)\big)^2\ , \tag{10}$$

where X represents the original image and Y is the denoised image. The ENL is defined as [20]

$$ENL(I) = \frac{1}{\beta^2}\,, \tag{11}$$

where β represents the standard deviation to mean ratio for correlated pixel. Specifically, the first experiment on simulated data is to determine the optimum wavelet scale for the technique. The experiment is run under the additive white Gaussian noise set up. Secondly, using the optimum wavelet scale, the performance of AMPT filter in reducing speckle noise is compared with other filters namely, Lee, boxcar, median and LMMSE. Finally, using real US images, the performance of AMPT is evaluated and compared in terms of ENL values. Fig 11 shows the three test images used for quantitative and qualitative comparison of different filters performance.

(a) (b) (c)

Figure 11: (a) Barbara Image. (b) Lena Image. (c) Sailboat Image.

4.1 Evaluation of AMPT Filter at Different Wavelet Scale

In this experiment, the test images, Barbara, Lena and sailboat are corrupted with additive white noise at different level of noise variance, ranging from 10 to 50. The size of test images used is 512 by 512. The PNSR values at different wavelet scale are tabulated in Table 2 which indicates wavelet of scale one as the best parameter for the AMPT filter to denoise the corrupted images and obtain the highest value of PNSR. The PNSR values obtained from each simulated images vary depending on the noise level and the wavelet scale. From this experiment, higher wavelet scale will caused the PNSR values to drop. Thus, the most optimum wavelet scale for AMPT technique is when the scale is equal to one.

Table 2 : Wavelet threshold scheme with different noise variance and scale

Scale		Scale=1	Scale=2	Scale=3	Scale=4
PNSR	PN	PNW	PNW	PNW	PNW
Barbara image					
σ=10	28.12	29.65	27.98	27.88	27.86
σ=20	22.12	25.68	24.88	24.85	24.83
σ=30	18.57	24.03	23.84	23.80	23.74
σ=40	16.08	22.98	23.26	23.24	23.21
σ=50	14.16	22.15	22.92	22.87	22.83
Lena image					
σ=10	28.13	32.87	32.84	32.84	32.82
σ=20	22.11	28.14	28.14	28.16	28.20
σ=30	18.60	27.82	27.79	27.82	27.83
σ=40	16.08	26.08	26.15	26.13	26.11
σ=50	14.14	24.68	24.62	24.74	24.62
Sailboat image					
σ=10	28.14	31.21	31.19	31.19	31.20
σ=20	22.11	28.14	28.14	28.16	28.20
σ=30	18.58	26.35	26.37	26.37	26.39
σ=40	16.10	25.03	24.96	24.96	25.01
σ=50	14.14	23.73	23.76	23.76	23.76

4.2 Evaluation of AMPT Filter with Simulated Speckle Noise

In this experiment, the multiplicative speckle noise is added to the test images and the PNSR value of the denoised images by different filters are evaluated and tabulated in Table 3. The experiment is run for 100 trials in order to obtain the average PNSR values of each filter. The result in Table 3 clearly shows that AMPT filter outperformed Lee, median, boxcar and LMMSE filters. Specifically, for Barbara image, AMPT filter gave the highest value of average PNSR gain which is 10 percent. While for Lena image and sailboat image, the average PNSR gain is 25 percent and 19 percent, respectively. For Lena image, improvement of PNSR recorded in each filters are slightly better. For visual interpretation of data obtained in Table 3, Graph 1, 2 and 3 are plotted. Generally, in terms of PNSR, AMPT filter demonstrated the highest performance, followed by median filter, boxcar filter, Lee filter and lastly LMMSE filter.

Table 3 : Comparison of PNSR of different denosing method corrupted by speckle noise

	Noisy Image	LMMSE Filter	Lee Filter	Boxcar Filter	Median Filter	AMPT Filter
Barbara Image						
σ =0.1	21.91	21.33	22.39	22.89	23.83	24.73
σ =0.05	24.92	24.50	22.48	23.90	24.49	27.47
σ =0.03	27.14	25.55	22.52	24.39	24.81	29.55
σ =0.02	28.90	27.00	22.54	24.65	24.99	30.81
Lena Image						
σ =0.1	21.68	23.85	25.85	24.77	28.13	29.75
σ =0.05	24.69	25.07	26.07	26.57	30.26	31.59
σ =0.03	26.91	25.13	26.17	27.57	31.59	32.27
σ =0.02	28.67	26.00	26.22	28.17	32.41	32.45
Sailboat Image						
σ =0.1	21.36	23.44	24.23	23.76	26.59	27.77
σ =0.05	24.37	24.41	24.41	25.23	28.14	29.61
σ =0.03	26.59	25.48	24.48	26.00	28.99	30.56
σ =0.02	28.35	25.51	24.51	26.45	29.52	31.07

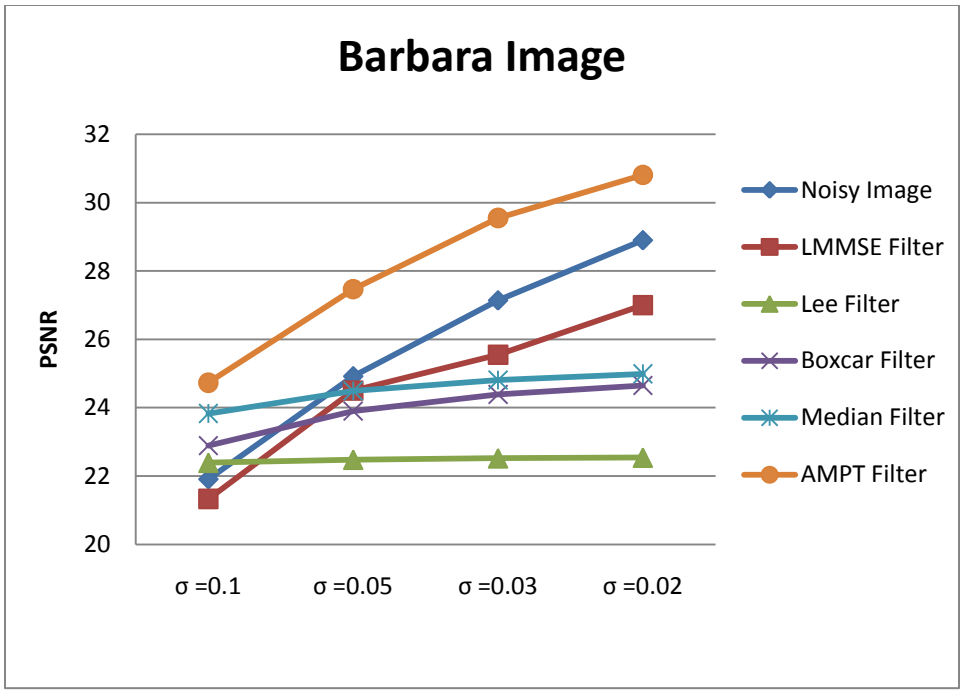

Graph 1: PNSR values of Barbara image

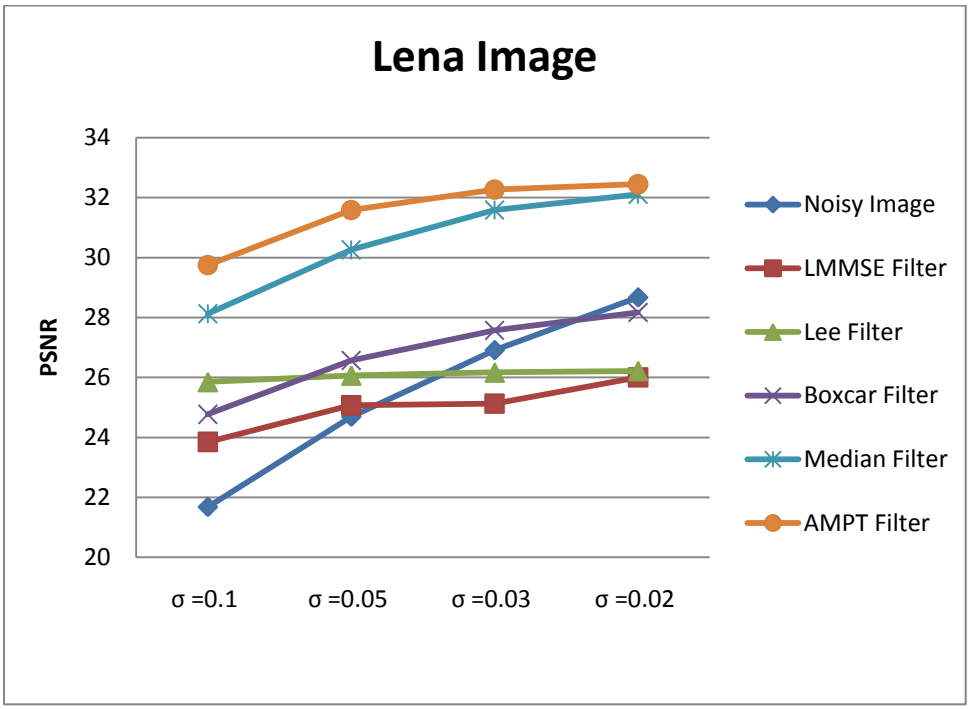

Graph 2: PNSR values of Lena image

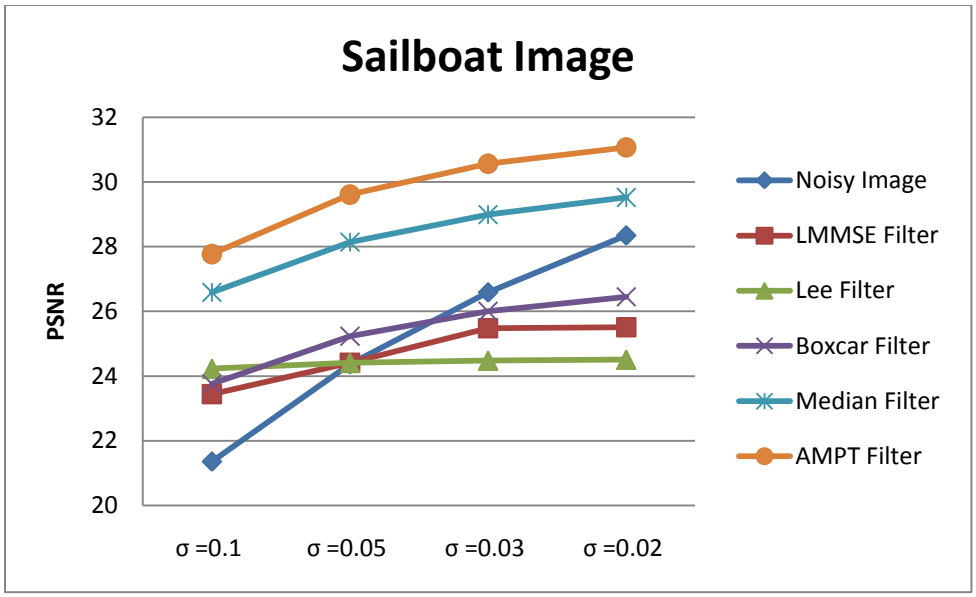

Graph 3: PNSR values of Sailboat image

On average, the PNSR performance of each filter can be summarized and plotted as shown in Graph 4. AMPT filter shows the highest gain value which is 1.22 times the noisy one, whereas the median, boxcar, Lee and LMMSE filter gave an average gain of 1.17, 1.04, 1.01 and 0.99, respectively.

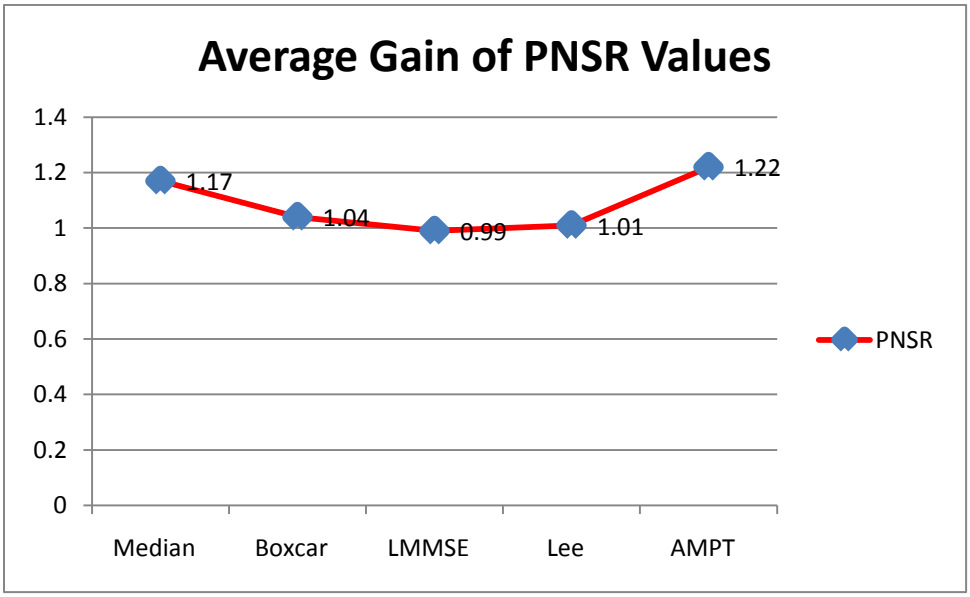

Graph 4 : Average gain of PNSR values in each filter

For visual inspection, Figs. 12, 13 and 14 illustrated zoom-in-images performance of the adaptive filters and the proposed technique on the employed simulation images. Fig. 12 shows the despeckling result of Barbara image that has been corrupted with speckle noise at noise variance of 0.1. In Fig. 12(c) and 12(d), zoom-in-image presented by boxcar filter and median filter shows that these denoising techniques did not smoothens the background noise effectively and retains much noise compared to other filters. In Fig 12(f), the image is denoised by using Lee filter with a size window of 5 by 5. Lee filter give good speckle suppression performance and almost 80 percent of the speckle noise is removed. However, the image is over smoothed and gives blurring effect. Some subtle details of the image are lost during the filtering process and the edge features are not effectively preserved. For instance, the plaid pattern of the table cloth and the scarf wrapped around Barbara appeared to be blurred and unclear. Besides, Lee filter 5 by 5 also causes the image to form a solid line surrounded the image. Fig. 12(g) shows the result of using AMPT technique with the same values of corrupted noise added. AMPT technique shows a good job in suppressing the effect of the speckle noise. Some of the noise are still retains in the image but the images are closely resemble the original image and less blurring compared to the Lee and LMMSE filter.

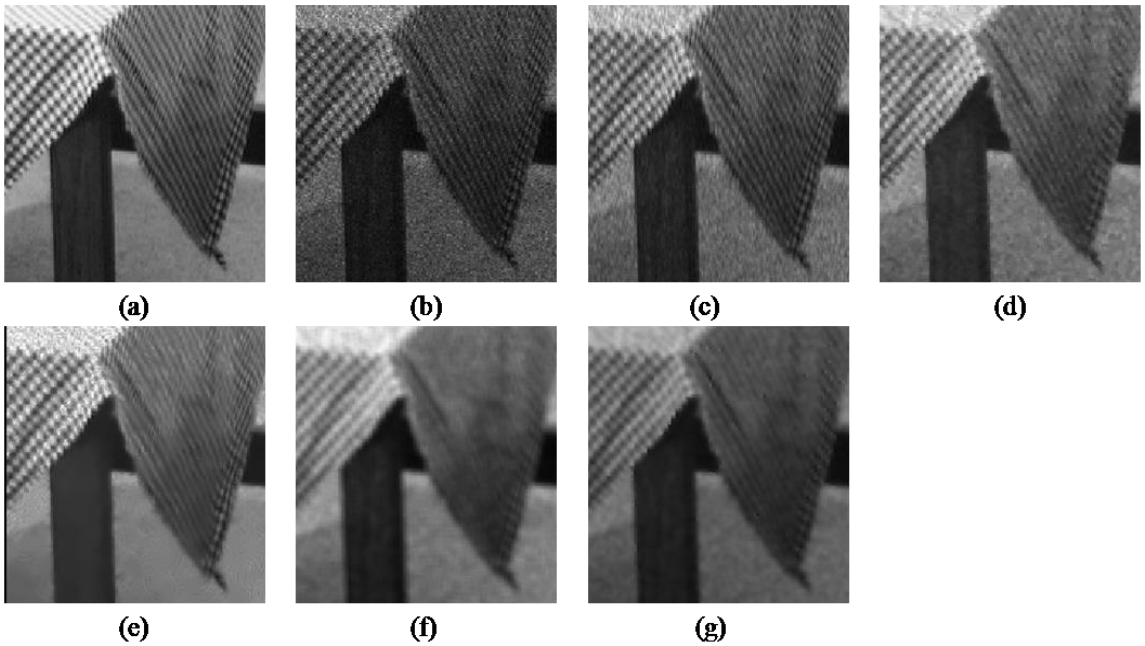

Figure 12: Zoom in of Barbara test image at noise level of 0.1. (a) Noise-free image. (b) Noisy image (PNSR=21.91). (c) Boxcar Filter (PNSR=22.89). (d) Median Filter (PNSR=23.83). (e) LMMSE Filter (PNSR=21.33). (f) Lee Filter (PNSR=22.39). (g) AMPT Filter (PNSR=24.73)

Similar to Barbara test image, despeckling the noisy image of Lena shows almost the same quality of result and is illustrated in Fig. 13. In this Fig.13, the zoom-in-image of Lena is focused at the fur on her hat. The AMPT technique presented the best visual performance by removing the speckle noise while maintaining the texture of the image. The qualitative comparison of each denoising scheme can be seen clearly in the Fig. 13 below.

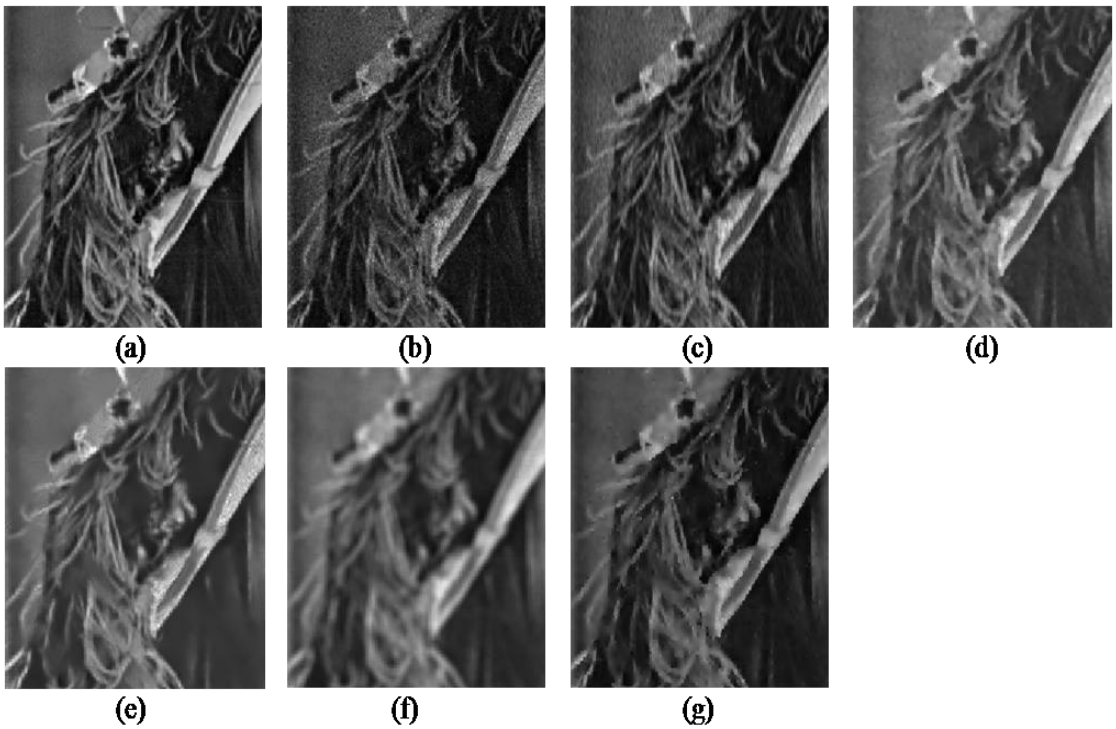

Figure 13: Zoom in of Lena test image at noise level of 0.1.
(a) Noise-free image. (b) Noisy image (PNSR=21.68). (c) Boxcar Filter (PNSR=24.77). (d) Median Filter (PNSR=28.13). (e) LMMSE Filter (PNSR=23.85). (f) Lee Filter (PNSR=25.85). (g) AMPT Filter (PNSR=29.75).

From this experiment, the performance of AMPT technique is better and gives a significant difference in terms of preserving the features of the images compared to others. The image denoised with AMPT is sharper and the recognition is better defined. As example, Fig. 14(g) shows the image of sailboat that has been denoised with AMPT. The image has many solid lines representing ropes and poles on the sail boat which are still clearer even after the despeckling process. The letters at the wall of the sailboat image can be clearly seen compared to the letters at the wall of the sailboat image filtered by median, Lee and LMMSE filter in Fig. 14(d-f).

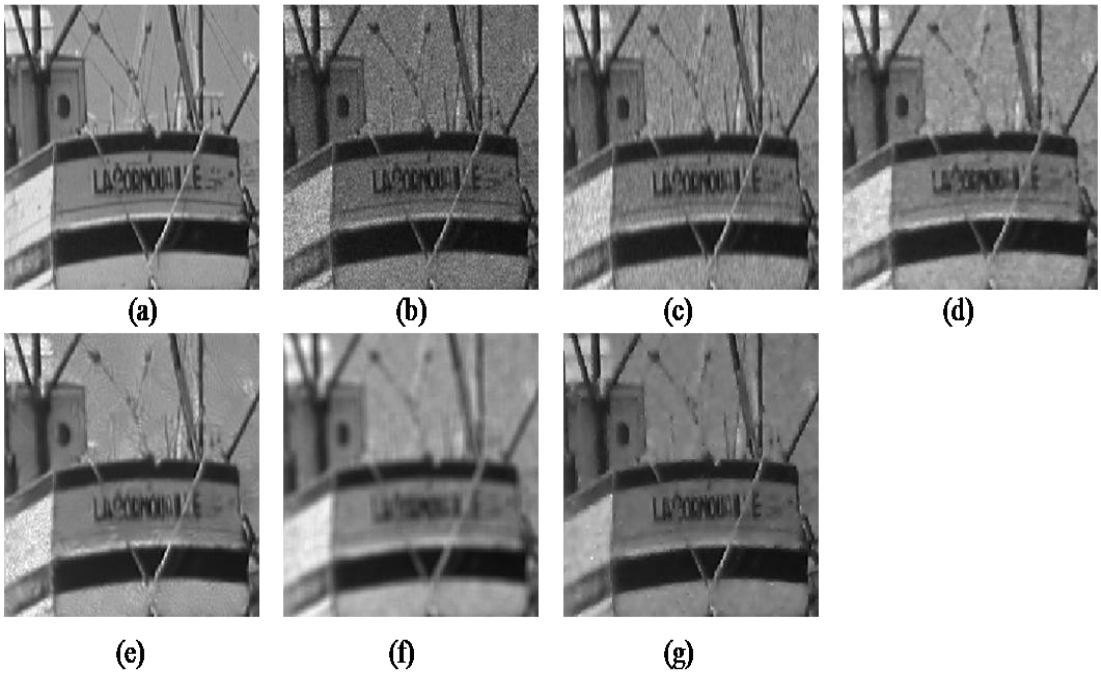

Figure 14: Zoom in of sailboat test image at noise level of 0.1. (a) Noise-free image. (b) Noisy image (PNSR=21.36). (c) Boxcar Filter (PNSR=23.76). (d) Median Filter (PNSR=26.59). (e) LMMSE Filter (PNSR=23.44). (f) Lee Filter (PNSR=24.23). (g) AMPT Filter (PNSR=27.77).

4.2 Evaluation of AMPT Filter using Real US Images

In this experiment, the real US images of fetus, breast, vena cava and liver images are been used to observe the performance of different filters on medical images. The size of US images used is 512 by 512 for fetus image, 412 by 412 for breast image, 328 by 328 for vena cava image and 250 by 250 for liver image. The desired regions of interest for calculating ENL value are highlighted in Fig. 15. The results obtained for each region are tabulated in Table 4.

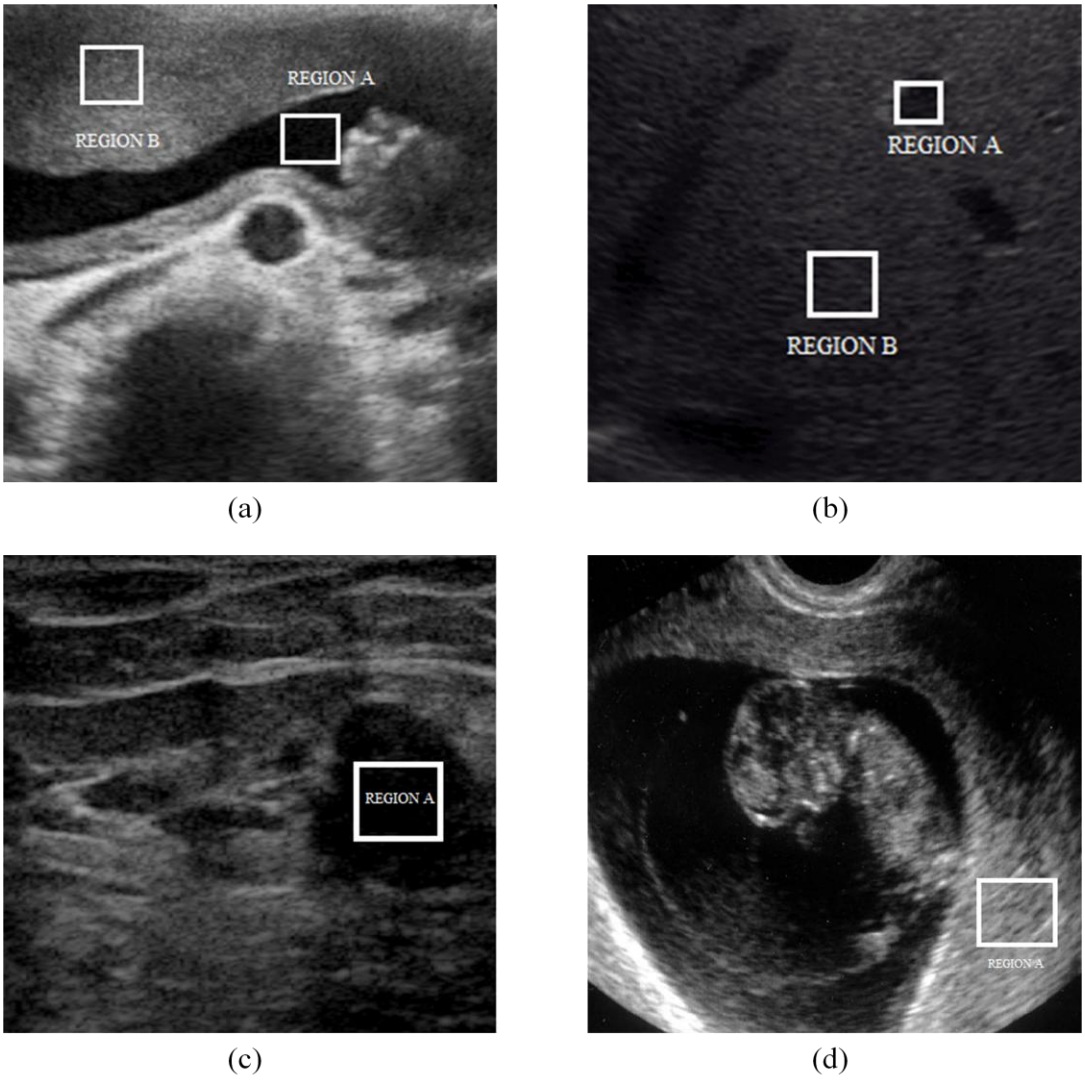

Figure 15: The desired regions of interest for calculating ENL value.
(a) Vena cava Image (b) Liver Image (c) Breast Image (d) Fetus Image

Table 4 : The ENL values of different US images.
(a) Vena cava image. (b) Liver image. (c) Breast image. (d) Fetus image

Technique	Vena cava	
	Region A	Region B
Original	4.25	20.51
Median	6.71	24.87
Boxcar	7.39	24.02
LMMSE	4.96	21.27
Lee	16.16	29.48
AMPT	7.59	27.89

(a)

Technique	Liver	
	Region A	Region B
Original	8.30	16.14
Median	9.68	24.52
Boxcar	9.57	32.40
LMMSE	8.57	17.16
Lee	11.97	70.64
AMPT	11.97	48.04

(b)

Technique	Breast
	Region A
Original	0.07
Median	0.06
Boxcar	0.13
LMMSE	0.09
Lee	0.24
AMPT	1.53

(c)

Technique	Fetus
	Region A
Original	73.18
Median	85.16
Boxcar	83.87
LMMSE	74.09
Lee	120.00
AMPT	105.80

(d)

From the Table 4, the performance of each filter in term of ENL values which indicates the ability of each filter to suppress the speckle noise in the desired region can be observed. In vena cava and liver image, two homogeneous regions are used to calculate the ENL while for breast and fetus image only one homogeneous region is used. On average, the performance gain of AMPT, Lee, median, boxcar and LMMSE filter is around 1.8, 2.67, 1.25, 1.5 and 0.97 times the noisy one, respectively. Graph 5 illustrated the average performance gain of each filter. In term of quantity measurement, Lee filter shows the highest performance and followed by AMPT filter. Though Lee filter outperformed AMPT filter in term of ENL values, the robustness of Lee technique still need to be inspect in other point of view.

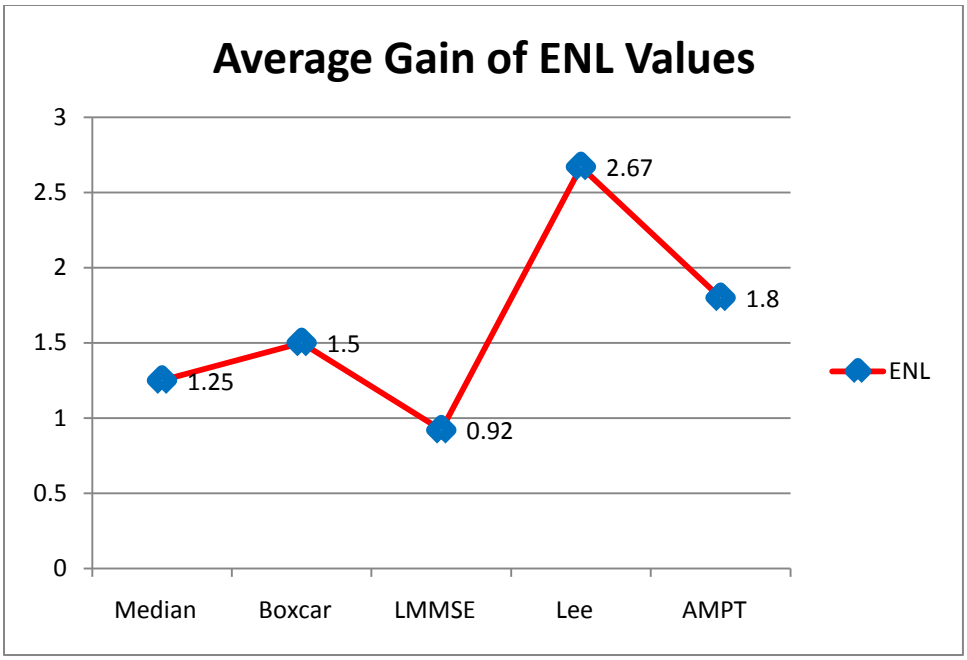

Graph 5: Average gain of ENL values in each filter

As mention previously, the performance of each filter is not only evaluate in term of quantity measurement but are evaluated and compared from a qualitative aspect as well. For this purpose, the visual performances of each filter on real US images are illustrated in Figs 16, 17, 18 and 19. Fig 16 shows the image of noisy vena cava and denoised version of vena cava image by using different type of filters. From this figure, it can be clearly seen that, the proposed technique, AMPT reduced the noise effectively and retained the important details of the image. Besides, AMPT filter preserved the contrast of the image very well compared to the other filters. In term of suppression of noise, LMMSE and Lee filter also show a good performance but the noise is overly smoothed out resulting in blurred image. On the other hand, the image obtained by using median and boxcar filter is still noisy

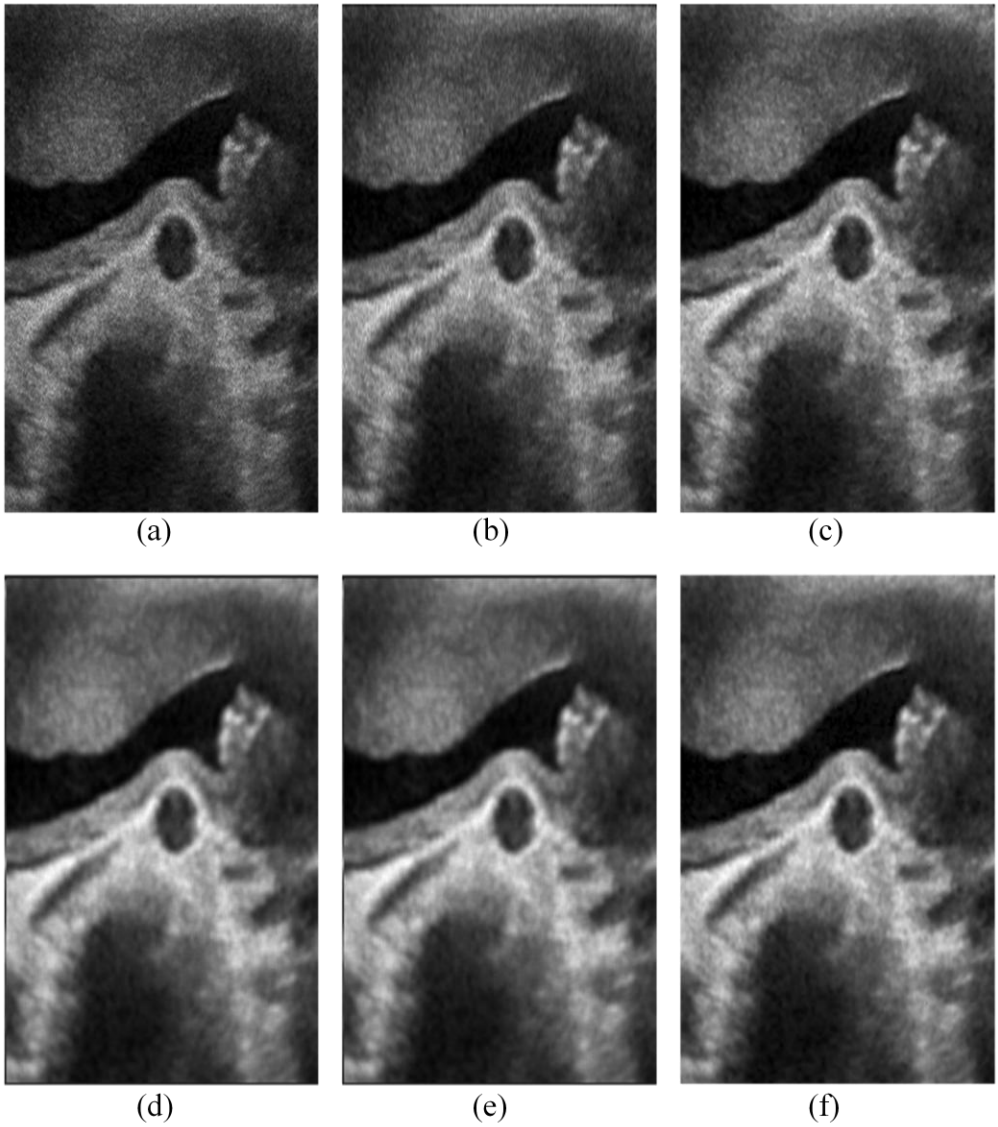

Figure 16 : Denoised image of vena cava.
(a) Noisy image (ENL Region A =4.25, ENL Region B= 20.51). (b) Boxcar Filter (ENL Region A =7.39, ENL Region B =24.02).
(c) Median Filter (ENL Region A =6.71, Region B =24.87). (d) LMMSE Filter (ENL Region A =4.96, Region B =21.27). (e) Lee Filter (ENL Region A =16.16, Region B =29.48). (f) AMPT Filter (ENL Region A =7.59, Region B =27.89).

The effectiveness of AMPT filter is further demonstrated in Fig 17, which also shows the despeckling of noise by the boxcar, median, LMMSE and Lee filter for fetus image.

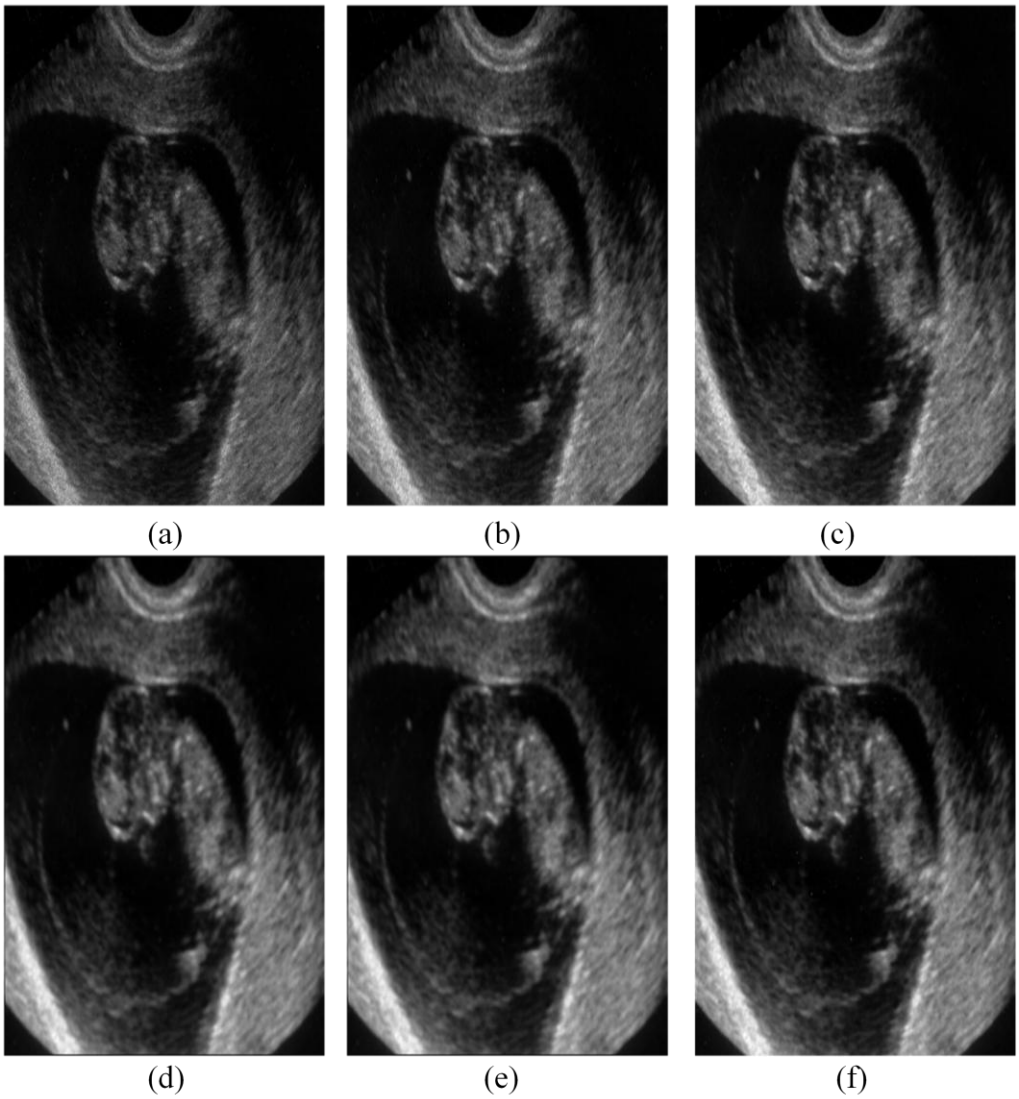

Figure 17: Denoised image of fetus.
(a) Noisy image (ENL =73.18). (b) Boxcar Filter (ENL =83.87).
(c) Median Filter (ENL =85.16). (d) LMMSE Filter (ENL =74.09). (e) Lee Filter (ENL =120). (f) AMPT Filter (ENL =105.8).

In Fig 18, the denoised image of a breast tissue is shown as below. From this figure, the preservation of the image contrast can be clearly observed. Here, boxcar and AMPT filter still maintained the contrast of the original image whereas the contrast in denoised image of median, LMMSE and Lee started to lessen.

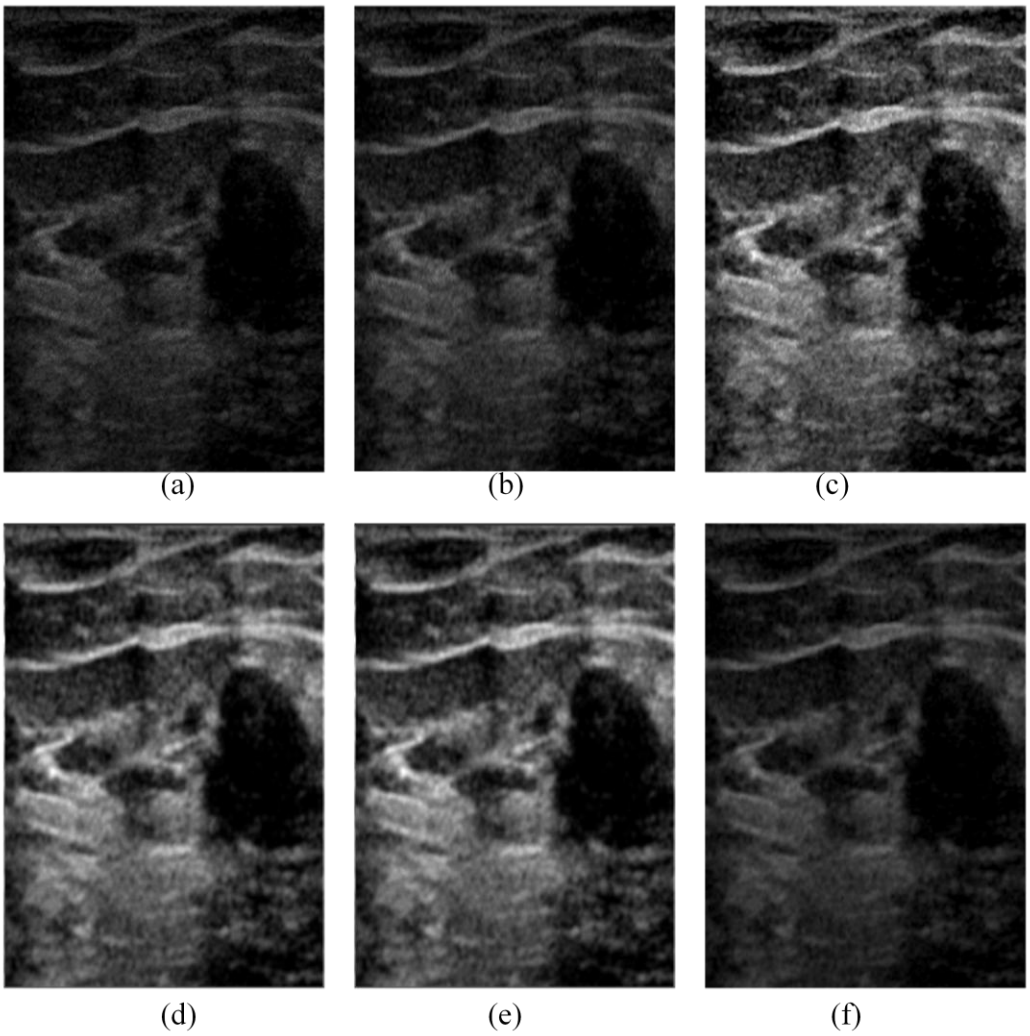

Figure 18: Denoised image of breast tissue.
(a) Noisy image (ENL =0.07). (b) Boxcar Filter (ENL =0.13).
(c) Median Filter (ENL =0.06). (d) LMMSE Filter (ENL =0.09). (e) Lee Filter (ENL =0.24). (f) AMPT Filter (ENL =1.53).

In Fig 19, the denoised image of US liver image is illustrated as below. In this figure, the blurring effect caused by the denoising process can be observed. Denoised image obtained from LMMSE and Lee filter are smoothed but it gave some blurring effect. Similarly, the image produced by the AMPT filter also shows some blurring effect but less blurred compared to LMMSE and Lee filter. Whereas for boxcar and median image, the image are noisy but less blurred.

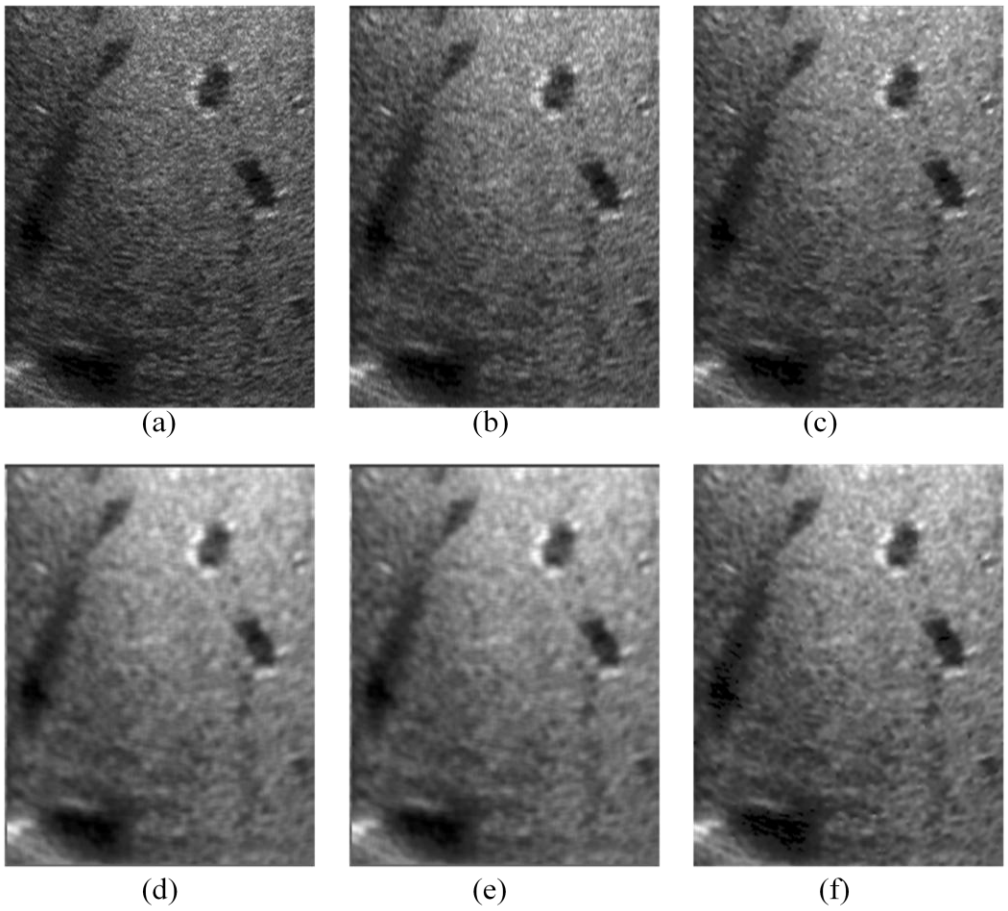

Figure 19: Denoised image of liver.
(a) Noisy image (ENL Region A =8.30, Region B = 16.14). (b) Boxcar Filter (ENL Region A =9.57, Region B = 32.40).
(c) Median Filter (ENL Region A =9.68, Region B = 24.52). (d) LMMSE Filter (ENL Region A =8.57, Region B = 17.16). (e) Lee Filter (ENL Region A =11.97, Region B = 70.64). (f) AMPT Filter (ENL Region A =11.97, Region B = 48.04).

From the denoised US image of vena cava, breast tissue, fetus and liver, the robustness of each filter are further verified. Even though AMPT filter shows slightly lower performance in term of ENL metric, but in term qualitative aspect, AMPT surpassed other filters in suppressing the speckle noise, preserving the contrast and image details. Whereas, Lee filter obtained high value of ENL but the quality of denoised image are defeated by AMPT as the image produced are over smoothed and blurred. In addition, the results obtained from simulation test images proved the ability of AMPT technique as a good despeckling filter. The selection of noise removal filter need to be used, varies depending on the type application. For US application, some denoising techniques are not preferable because these filters are too sophisticated and may destroy some useful and relevant information of the image. Therefore, it is important to choose denoising tool which can secure the conservation of image details while smoothing out the speckle noise. Preferring to the US application, AMPT technique can be used and stand as a dominant denoising tool.

The proposed technique is also computationally fast compared to Lee and LMMSE technique. On average, it takes less than 4 seconds to process the image depending on the size of image. This experiment is carried out on a 2.4 GHz Intel (R) Core ™ i3 CPU computer with 2.00 GB RAM, and 64-bit operating system.

CHAPTER 5

CONCLUSION AND FUTURE WORK

In this paper, speckle noise denoising scheme using adaptive multiscale product thresholding (AMPT) is introduced and implemented in the simulation and real US image. From the simulation results, AMPT shows better performance in term of PNSR values and visual quality while removing a substantial amount of noise, the details and sharpness of the original image is maintained. The evaluation of AMPT filter using real US images shows proved that AMPT technique is capable of reducing speckle noise in homogeneous region of US image with less blurring effect while preserving contrast and image details such as edges and subtle features. On average, the performance gain of AMPT in terms of PNSR and ENL is around 1.22 times and 1.8 times the noisy one, respectively. Thus, it is believed that the implementation of this technique in medical ultrasound imaging will enhance the quality of US images produced.

In the AMPT filter, the wavelet thresholding discard the small value of wavelet product coefficient because it is treated as noise. This process however, may results in removal of some important tissue detail in ultrasound images. As future work, further investigation should be conducted on the statistical property of the US images and how to incorporate this information into the AMPT filtering process. It is expected that with additional statistical information, the filtering performance will be further improved.

REFERENCES

[1] C. C. Freudenrich. *How Ultrasound Works*. Available: http://www.physics.utoronto.ca/~jharlow/teaching/phy138_0708/lec04/ultrasoundx.htm

[2] S. K. Narayanan and R. Wahidabanu, "A view on despeckling in ultrasound imaging," vol. 2, 2009.

[3] S. Sudha, G. Suresh, and R. Sukanesh, "Speckle noise reduction in ultrasound images by wavelet thresholding based on weighted variance," *International journal of computer theory and engineering*, vol. 1, pp. 1793-8201, 2009.

[4] Z. Changming, N. Jun, L. Yanbo, and G. Guochang, "Speckle Noise Suppression Techniques for Ultrasound Images," in *Internet Computing for Science and Engineering (ICICSE), 2009 Fourth International Conference on*, 2009, pp. 122-125.

[5] P. Bao and D. Zhang, "Noise reduction for magnetic resonance images via adaptive multiscale products thresholding," *Medical Imaging, IEEE Transactions on*, vol. 22, pp. 1089-1099, 2003.

[6] R. C. Gonzalez, *Digital Image Processing*: Pearson Education, 2009.

[7] L. Zhang, X. Li, and D. Zhang, "Image denoising and zooming under the linear minimum mean square-error estimation framework," *Image Processing, IET*, vol. 6, pp. 273-283, 2012.

[8] M. Misiti, Y. Misiti, G. Oppenheim, and J. M. Poggi, *Wavelets and their Applications*: Wiley, 2013.

[9] Y. Qin, B. Tang, and J. Wang, "Higher-density dyadic wavelet transform and its application," *Mechanical Systems and Signal Processing*, vol. 24, pp. 823-834, 4// 2010.

[10] J. Duan and I. S. Oweis, "Dyadic wavelet analysis of PDA signals," *Soil Dynamics and Earthquake Engineering*, vol. 25, pp. 661-677, 8// 2005.

[11] M. I. H. Bhuiyan, M. O. Ahmad, and M. N. S. Swamy, "Spatially adaptive thresholding in wavelet domain for despeckling of ultrasound images," *Image Processing, IET*, vol. 3, pp. 147-162, 2009.

[12] S. G. Chang, Y. Bin, and M. Vetterli, "Adaptive wavelet thresholding for image denoising and compression," *Image Processing, IEEE Transactions on,* vol. 9, pp. 1532-1546, 2000.

[13] L. Kaur, S. Gupta, and R. Chauhan, "Image denoising using wavelet thresholding," in *Proceedings of the Third Indian Conference on Computer Vision, Graphics & Image Processing*, 2002, pp. 1522-1531.

[14] S. Wang, J. Zhou, J. Li, and L. Jiao, "Speckle Noise Reduction for Ultrasound Images via Adaptive Neighborhood Accumulated Multi-scale Products Thresholding," in *Intelligent Science and Intelligent Data Engineering*. vol. 7202, Y. Zhang, Z.-H. Zhou, C. Zhang, and Y. Li, Eds., ed: Springer Berlin Heidelberg, 2012, pp. 397-404.

[15] D. L. Donoho and J. M. Johnstone, "Ideal spatial adaptation by wavelet shrinkage," *Biometrika,* vol. 81, pp. 425-455, 1994.

[16] P. Quan, D. Zhang, D. Guanzhong, and Z. Hongcai, "Two denoising methods by wavelet transform," *Signal Processing, IEEE Transactions on,* vol. 47, pp. 3401-3406, 1999.

[17] B. M. Sadler and A. Swami, "Analysis of multiscale products for step detection and estimation," *Information Theory, IEEE Transactions on,* vol. 45, pp. 1043-1051, 1999.

[18] Y. Xu, J. B. Weaver, D. M. Healy, Jr., and J. Lu, "Wavelet transform domain filters: a spatially selective noise filtration technique," *Image Processing, IEEE Transactions on,* vol. 3, pp. 747-758, 1994.

[19] S. Mallat and S. Zhong, "Characterization of signals from multiscale edges," *Pattern Analysis and Machine Intelligence, IEEE Transactions on,* vol. 14, pp. 710-732, 1992.

[20] J. S. Lee and E. Pottier, *Polarimetric Radar Imaging: From Basics to Applications*: Taylor & Francis, 2009.

APPENDIX

A: MATLAB Code

a) MATLAB code (main part) used for simulation of test images

```
clc;clear all; close all
x     = double(imread('lena.png'));
x     = x(:,:,1);
[K,L] = size(x);
%%%%%%%%%%%%%%%---- Adding speckle noise ----%%%%%%%%%%%%%
v    = 0.1;
n1   = specklegengam(K,L,1/v);
n2   = specklegengam(K,L,1/v);%n10   = specklegengam(K,L,1/v);
n3   = specklegengam(K,L,1/v);%n11   = specklegengam(K,L,1/v);
n4   = specklegengam(K,L,1/v);%n12   = specklegengam(K,L,1/v);
n    = (n1+n2+n3+n4)/4; % 4-look data
y    = x.*n;
yy   = relog(y);
ly   = log10(yy);
PN   = PSNR(x,y);

%%%%%%%%%%%%%%%---- Variance estimation ----%%%%%%%%%%%%%
wv    ='db4' ;
level = 1; % db1, db4, sym4, bior6.8
ftype = wv;
[C,S] = wavedec2(ly,level,ftype);
var   = length(C)-S(size(S,1)-1,1)^2+1;
ve   = median(abs(C(var:length(C))))/0.6745;
%%%%%%%%%%%%%%%---- Boxcar ----%%%%%%%%%%%%%
 N = 3;
 B = filter(boxcar(N)/N,1,y);
 PB = PSNR(B,x);
%%%%%%%%%%%%%%%---- Median filter ----%%%%%%%%%%%%%
M = medfilt2(y);
PNM  = PSNR(M,x); %  PNSR of median
%%%%%%%%%%%%%%%---- LMMSE filter ----%%%%%%%%%%%%%
lmmse = Lmmse_US(x);
PLMMSE   = PSNR(lmmse,y)%  PNSR of LMMSE
%%%%%%%%%%%%%%%---- Lee filter ----%%%%%%%%%%%%%
Le5 = lee5by5(y);
PL   = PSNR(Le5,x); %  PNSR of Lee
%%%%%%%%%%%%%%%---- AMPT ----%%%%%%%%%%%%%
Wlt = ZhangW(ly,v);
Wlt = 10.^Wlt;
PNW  = PSNR(Wlt,x); %  PNSR of AMPT
out = [PN,PB,PNM,PLMMSE,PL,PNW]
%%%%%%%%%%%%%%%---- Test images ----%%%%%%%%%%%%%
figure; imshow(x,[]);xlabel('Noise-free')
figure; imshow(y,[]);xlabel('Noisy')
figure;imshow(B,[ ]);xlabel('Boxcar')
figure; imshow(M,[]);xlabel('Median')
figure;imshow(lmmse,[ ]);xlabel('LMMSE')
figure;imshow(Le5,[ ]);xlabel('Lee5by5')
figure; imshow(Wlt,[]);xlabel('AMPT')
```

b) MATLAB code for AMPT Technique

```
function out = ZhangW(imagn,v)
sca=1;
[wr,wc,ss,m]=wt2d(imagn,sca);
[corr,corc]=compcor2d(wr,wc);

%%%%%%%%%%%%%%%%%%%%%%%%%%%%%%%%%%%%%%%%%%%%%%%%%%%%%%%%%%%%%%%%
rimat=th_w2d(wr,wc,ss,v,m);%%%do the traditional thresholding

%%%% the scale correlation thresholding
[sca,n,nn]=size(wr);

th=getth2d(sca);
c=15;
for i=1:sca-1
   wrt=reshape(wr(i,:,:),n,n);
   corrt=reshape(corr(i,:,:),n,n);
   mask=(corrt>c*v^2*th(i));
   iwr(i,:,:)=wrt.*mask;

   wct=reshape(wc(i,:,:),n,n);
   corct=reshape(corc(i,:,:),n,n);
   mask=(corct>c*v^2*th(i));
   iwc(i,:,:)=wct.*mask;
end

nf=normf2d(sca);
wrt=reshape(wr(sca,:,:),n,n);
iwr(sca,:,:)=wrt.*(abs(wrt)>3.*v*nf(sca));
wct=reshape(wc(sca,:,:),n,n);
iwc(sca,:,:)=wct.*(abs(wct)>3.*v*nf(sca));

out=iwt2d(iwr,iwc,ss,m);
```

```
function [wwr,wwc,ss,m]=wt2d(image,sca)

%%%2D dyanic wavelet transform%%%%%%%%%%

%image------input image
%sca--------transform scale number

%wwr--------row output
%wwc--------column output
%ss---------smoothed image
%m----------extended point number

%!!! The image should be square

J=sca;
[n,m]=size(image);
if m>64
   m=64;
end

%%%%%%%%reform the image%%%%%%%%%%%%%%%%%%
ima=zeros(2*m+n,2*m+n);
ima(m+1:m+n,:)=[image(:,m:-1:1) image image(:,n:-1:n-m+1)];
ima(1:m,m+1:m+n)=image(m:-1:1,:);
ima(m+n+1:2*m+n,m+1:m+n)=image(n:-1:n-m+1,:);
%%%%%%%%%%%%%%%%%%%%%%%%%%%%%%%%%%%%%%%%%%
clear image;

j=0;
while j<J
   rt=conv2(ima,getg(j));
   wwr(j+1,:,:)=rt(:,128:128+n+2*m-1);
   ct=conv2(ima,getg(j)');
   wwc(j+1,:,:)=ct(128:128+n+2*m-1,:);

   st=conv2(ima,geth(j));
   st=st(:,128:128+n+2*m-1);
   ima=conv2(st,geth(j)');
   ima=ima(128:128+n+2*m-1,:);
   j=j+1;
end

ss=ima;

return;
```

```
function a=geth(i)

%%%get the low pass filter%%%%%

a=zeros(1,256);
a(128)=0.375;
a(128-2^i)=0.125;
a(128+2^i)=0.375;
a(128+2*2^i)=0.125;

return;

=====================================================================


function a=getg(i)

%%%get the high pass filter%%%%%

a=zeros(1,256);
a(128)=-2.0;
a(128+2^i)=2.0;


return;
=====================================================================

function tth=getth2d(sca)

%%%%compute ||F1||||F2||sigma_z1^2%%%%

%sca-----scale number
%tth-----the output, a vector of length sca, consists of the threshold
at scale i=1,2,...,sca

nf=normf2d(sca+1);
[sigma_z1,sigma_z2]=getsigma2d(sca);

for i=1:sca
   tth(i)=(nf(i)*nf(i+1)*sigma_z1(i));
end

return;

=============================================================


function nf=normf2d(sca);

%%%%compute ||H0*H0'*H1*H1'...*Grm||%%%%%%%

%sca----scale number
%nf-----the output in row or column direction, a vector of length sca
```

```
th=1;

for i=0:sca-1
  tg=conv(th,getg(i));
  nf(i+1)=norm(tg)*norm(th);
  th=conv(th,geth(i));
end
```

==========

```
function rima=iwt2d(wwr,wwc,ss,m)

%%%backward dyadic wavelet transform%%%%%%
%wwr--------row part
%wwc--------column part
%ss---------smoothed image
%m----------extended point number

%rima-----reconstructed image

[J,n,nn]=size(wwr);

j=J;
while j>0
   twwr=reshape(wwr(j,:,:),n,n);
   twwr=conv2(twwr,getk(j-1));
   twwr=twwr(:,128:128+n-1);
   twwr=conv2(twwr,getl(j-1)');
   twwr=twwr(128:128+n-1,:);

   twwc=reshape(wwc(j,:,:),n,n);
   twwc=conv2(twwc,getl(j-1));
   twwc=twwc(:,128:128+n-1);
   twwc=conv2(twwc,getk(j-1)');
   twwc=twwc(128:128+n-1,:);

   ss=conv2(ss,getnh(j-1));
   ss=ss(:,128:128+n-1);
   ss=conv2(ss,getnh(j-1)');
   ss=ss(128:128+n-1,:)+twwr+twwc;

   j=j-1;

end

rima=ss(m+1:n-m,m+1:n-m);
```

B: Gantt Chart (with key milestones)

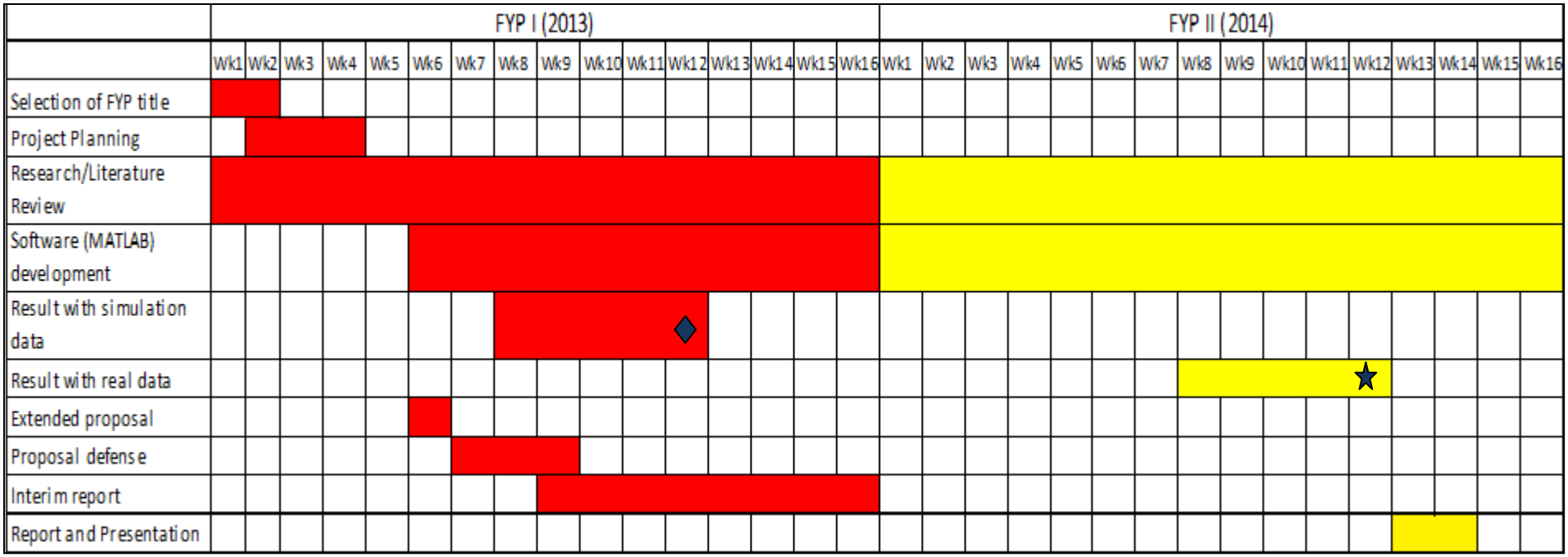

◆ Milestones 1- Result with simulation data

★ Milestones 2- Result with real data